

Research Article

Inerting Strategy for a Demonstration-Scale Hot Cell Facility Based on Experiences from Pilot-Scale Argon Cell Facility Operation and CFD Analysis

Seungnam Yu , Jaehoon Lim , Ilje Cho , and Jonghui Han 

Korea Atomic Energy Research Institute, 111, Daedeok-daero 989 Beon-Gil, Yuseong-Gu, Daejeon 34057, Republic of Korea

Correspondence should be addressed to Seungnam Yu; snyu@kaeri.re.kr

Received 5 March 2021; Accepted 28 May 2021; Published 24 June 2021

Academic Editor: Massimo Zucchetti

Copyright © 2021 Seungnam Yu et al. This is an open access article distributed under the Creative Commons Attribution License, which permits unrestricted use, distribution, and reproduction in any medium, provided the original work is properly cited.

Pyroprocessing is being developed at Korea Atomic Energy Research Institute (KAERI), and in recent years, all process equipment required for integrated processes have been examined in the PyRoprocess-integrated Inactive DEMonstration (PRIDE) facility. Based on the successful operation of a pilot-scale facility, a conceptual design for this scale-up facility was actualized. Implementing a “demonstration-scale” hot cell facility is challenging as it is intended to supersede PRIDE and satisfy the increased requirements of larger-scale facilities. This study focused on an inerting strategy for a larger-scale (demonstration-scale) hot cell facility to achieve conditions equivalent to those in a pilot-scale gas-tight argon cell facility. The study applies the inerting strategy to a demonstration-scale hot cell facility beyond that of the currently existing pilot-scale hot cell facility and performs computational fluid dynamics (CFD) simulation with various flow rates to determine an appropriate approach for inerting the target facility. To this end, practical constraints on the simulation are introduced based on experiences from the existing pilot-scale facility. The results show that the purging flow rate should be accurately predicted, and a variable flow rate should be applied to achieve hot cell inerting effectively. The required purging time and amount of inerting source are essential factors in the larger-scale hot cell facility. The study results can be helpful in the design of large hot cell facilities operated under inert conditions.

1. Introduction

One of the most effective methods of reducing uncertainty when scaling a process is to perform bench-scale research on actual feed material, particularly when expecting that the feedstock will be subject to campaign-specific variance. This is critical when dealing with electrometallurgical and electrochemical processes, in which trace impurities can affect the entire process. Korea Atomic Energy Research Institute (KAERI) has been developing pyroprocessing technology since 1997, and it has performed core concept development, bench-scale tests, and lab-scale demonstrations since 2006.

From 2007 to 2011, it conducted the design and construction of a pilot-scale integrated system, called the PyRoprocess-integrated Inactive DEMonstration (PRIDE) facility (Figure 1), with an annual capacity of 10 tons for batch process using inactive simulants with depleted

uranium [1–4]. Pyroprocessing should be performed under an inert atmosphere and involves head-end processes (i.e., decladding, voloxidation, and oxide feed preparation), electrochemical processes (i.e., electrolytic reduction, electrorefining, and electrowinning), and waste treatment processes [5, 6]. In recent years, all process equipment required for integrated processes have been examined in PRIDE under an argon atmosphere (Figure 2) [7–10].

Pilot plants serve as small-scale production systems to test practically and validate a production technology before commercialization. Generally, the primary motivation behind operating pilot plants is to understand and develop new technology. The lessons thus learned bring valuable experience and data that can help establish a safer, more efficient, and commercially viable larger- or full-scale production facility [11]. The differences between bench-scale, pilot-scale, and even demonstration-scale systems are strongly

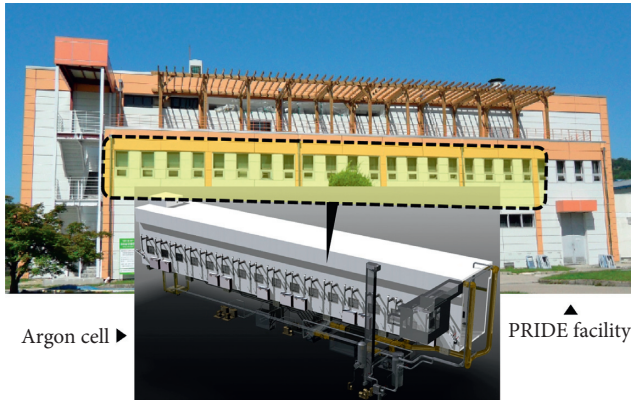


FIGURE 1: Isometric view of argon cell of PRIDE facility.

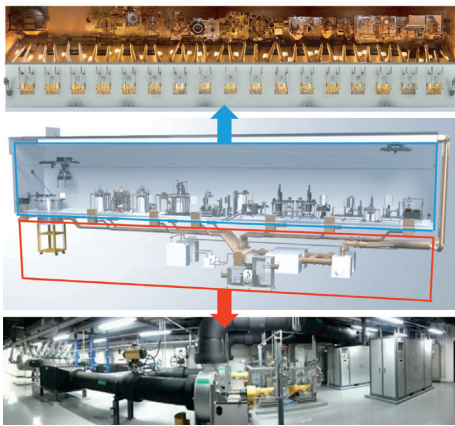


FIGURE 2: Argon circulation system for PRIDE facility (Top: Top view of argon cell, Middle: Cut view of argon cell, Bottom: Photo of argon circulation system operated under the argon cell).

influenced by industry and application. Some industries use pilot and demonstration plants interchangeably. The demonstration scale involves operating equipment at total commercial feed rates over extended periods to prove operational stability [12].

Recently, based on the successful operation of PRIDE in KAERI, a conceptual design for a scale-up facility was actualized. Implementing a “demonstration-scale” hot cell facility is challenging as it is intended to supersede PRIDE and satisfy the increased requirements of larger-scale processes. Essentially, this facility is required to process hazardous materials, such as spent nuclear fuel, which must be processed in a highly shielded area, namely, in a hot cell isolated from the operator’s working area. Moreover, an inert gas atmosphere must be maintained in pyroprocessing because it is inert to the lithium chloride and other materials in the electrolyte salt while preventing pyrophoric reactions of metal fuel. The considered facility must also achieve significantly increased annual production beyond that of the previous facility. This study focused on an inerting strategy for a larger-scale (demonstration-scale) hot cell facility to achieve conditions equivalent to those in the pilot-scale gas-tight argon cell facility. Facilities similar to PRIDE that require inerting conditions can be found in other research

institutes, as shown in Table 1. However, they have functional and structural differences from each other, such as in terms of the cell volume, degree of radiation hardness, and applications. Therefore, we had to find an appropriate purging method based on our experience of the existing pilot-scale facility operation, and we investigated the efficient and economic purging parameters for the initial inerting of the considered demonstration-scale facility.

2. Basic Considerations for Inerting Target Facility

2.1. Background. PRIDE is a pilot facility used to simulate integrated pyroprocessing at an engineering (pilot) scale in an inert atmosphere. The main operation facility is 40 m in length, 4.8 m in width, and 6.4 m in height. The utility systems are operated to maintain an inert atmosphere, and their operational requirements determine that the concentrations of oxygen and moisture be maintained below 50 ppm. Therefore, the following basic assumptions related to calculating the circulating flow of the inerting gas in PRIDE were made. First, the supply and discharge of the gas are performed until the hot cell’s undesired gas content decreases to less than 200 ppm, and then, the purification system is operated. Currently, there is no standard for the circulation rate of the atmospheric gas for the hot cell. Therefore, the circulation rate of a similar facility is applied to PRIDE, that is, a circulation rate of 16 times per hour. For reference, the air cell ventilates 1 to 30 times per hour [20].

2.2. Purging Gas Selection. Initially, nitrogen and argon were considered inert gas candidates for the target facility. Practically, there is no difference between nitrogen and argon when used to purge air or oxygen out from a closed space. Both are efficiently nonreactive; however, argon is less reactive than nitrogen, whereas nitrogen is much cheaper than argon. Furthermore, argon is in such a small percentage of the atmosphere that argon is often more expensive than nitrogen. From this economic aspect, nitrogen is preferred in some applications.

On the other hand, purging air with argon is faster because of the heavier mass of argon (40 g/mol) compared with that of air (28.9 g/mol), whereas the mass of nitrogen is slightly lower (28 g/mol) than that of air. Therefore, for large volumes of a hot cell, purging with nitrogen would require a longer time to be stabilized. Both gases can generate an inert atmosphere, remove oxygen and moisture, avoid corrosion, and create an anaerobic environment in a closed space. However, argon has an advantage in flushing out the initial air more efficiently on high-speed purging lines.

As mentioned above, the advantage of argon is the ease of purging because of its high weight. Argon has a density of 1.6 kg/m^3 , whereas nitrogen is 1.12 kg/m^3 ; it is approximately 40% heavier per cubic meter than nitrogen. Therefore, argon has many protective applications in iron, steel, and heat treatment industries, particularly in metals susceptible to nitriding when treated with a nitrogen-based atmosphere (which is another critical issue in pyroprocessing). Therefore, argon gas was selected as the purging media in this study.

TABLE 1: Comparison of specifications among experimental hot cells and gas-tight cells [13–19].

Contents	Facility names				
	FCF [13, 14]	HFEF [15, 16]	ACPF [17, 18]	PRIDE [19]	Target facility of this study
Cell volume	1,470 m ³ (argon cell)	1,473 m ³ (argon cell)	9.4 m ³ (argon cell)	1,230 m ³	7,560 m ³
Cell pressure (negative)	51–102 mmH ₂ O [13]	20–100 mmH ₂ O [15]	27–37 mmH ₂ O	10–200 mmH ₂ O	12–100 mmH ₂ O
Oxygen impurity	<60 ppm [14]	20–100 ppm [16]	<50 ppm	<50 ppm	<30 ppm
Water impurity	<60 ppm [14]	20–100 ppm [16]	<50 ppm	<50 ppm	<50 ppm

2.3. Purging Method Selection. The removal of the undesired gas, either air or process gas, is known as purging. The most common method of purging is replacing the undesired gas with a high-purity inert gas (purge gas) that does not react with either air or the process gas nor poses any other hazardous materials. Either displacement or dilution accomplishes replacement. In the displacement method, the undesired gas is replaced by a purge gas without intermixing them. Theoretically, this approach represents a fast and straightforward way of purging; however, in practice, it is hard to introduce a gas into a piping system without intermixing with the gas already existing in the hot cell. In the dilution method, the concentration of the undesired gas is reduced by accumulating the purge gas. The amount of undesired gas does not change, but as more purge gas is accumulated, the concentration of the undesired gas (percentage of the total amount of gas present) decreases. Individual use of displacement and dilution is a conceptual approach; practical purging methods generally employ a combination of them [21].

Displacement purging is performed by injecting inert gas into an open hot cell facility to displace an undesired gas with a low flow rate, for example, under 10 m/s. This method is used primarily when the H (height)/ A (area) ratio of the target facility is high. The inert gas should ideally have a higher density than the gas to be displaced. From a safety perspective, limiting oxygen concentration (L_{oxy}) is an essential parameter for inerting. For a specific air–inert gas mixture, the L_{oxy} represents the marginal concentration of oxygen in the target facility. Practical and operational experiences can determine the reasonable degree of L_{oxy} . Other control parameters include the properties of the gas, the geometry of the hot cell space being inerted, inlet and outlet port configurations, and flow velocity. An example of a geometrical parameter is the H/A ratio of the hot cell. The following is applied in this study [21].

$H/A < 1$: Dilution purging

$H/A > 10$: Displacement purging

H : Height of a container or cell

A : Area of a container or cell

Dilution purging involves injecting inert gas to lower the concentration of an undesired gas. This method is used when the target facility has a lower H/A ratio, as mentioned above. The best way to achieve a proper degree of mixing is to have wide spacing between the inlet and the outlet ports and select inert gas with a density similar to that of the undesired gas.

The purging gas, such as argon, squeezes the atmosphere out of the hot cell through the exhaust gas outlet. The quantity of argon required is higher than the capacity of the hot cell (generally, the amount of argon needed is approximately 3.5 times the capacity of the hot cell for dilution purging). However, dilution purging is challenging to be solely applied to inert the entire space of the hot cell because the corner zone is hard to be inerted completely using argon gas with this method.

More specifically, two methods are commonly employed as a practical application: continuous flow purging and cycle purging. Continuous flow purging is the continuous introduction of purge gas at one end of a piping system with the continuous removal of a mixture of the two gases from the far end. In simple techniques, such as tubing runs, the displacement effect is considerable for a large portion of the undesired gas rapidly driven out at the end of the tubing. However, in complex systems containing branches and dead-end cavities, the situation is considerably different because there is a slight displacement of purging gas. As a result, the dilution of the gas in these parts of a system has a slow process.

Cycle purging is an alternative way of introducing purge gas into a hot cell and venting the mixture of purge gas and undesired gas from the cell. The introduction of purge gas achieves dilution, and the amount of undesired gas is reduced by venting the mixture, leaving a lesser amount of the dilute mixture in the system. This process is repeated with increasing dilution through the pressurization/venting cycle. When the venting pressure is less than the atmospheric pressure, the procedure is referred to as vacuum-assisted cycle purging. The purging efficiency is improved by increasing the purge gas inlet pressure, reducing the venting pressure, and/or increasing the number of cycles. The performance can be further enhanced by appropriate system design, such as minimizing the branches and dead-end cavities [22].

3. Case Study of Existing Facility: PRIDE

3.1. Argon Circulation System of PRIDE. PRIDE was built to conduct a pilot-scale operation of pyroprocessing using a simulated nuclear material; this process requires the continuous removal of oxygen and moisture in the cell. Therefore, PRIDE has a two-way argon delivery system for initial purging and regular operation. In the typical operation case, the port of the upper part of the cell becomes the



FIGURE 3: Inside the area of PRIDE argon cell, including ports for argon flow.

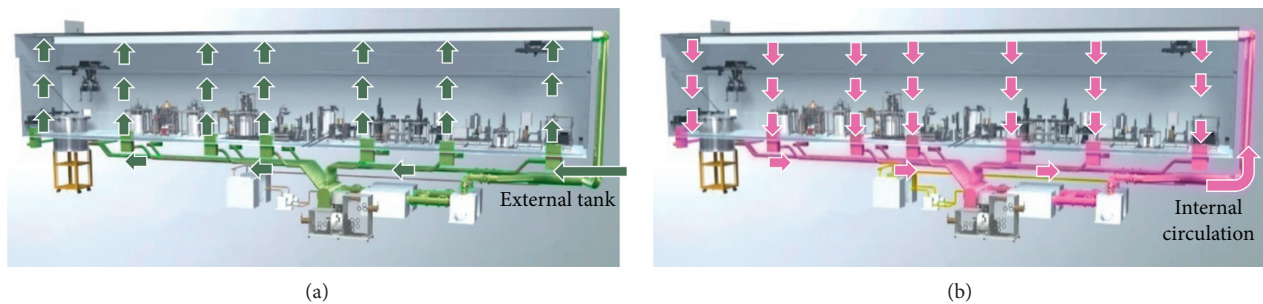


FIGURE 4: Argon flow for (a) initial purging and (b) regular operation.

inlet, and the lower part of the cell becomes the outlet for the weight of argon (Figures 3 and 4).

However, for an efficient initial purging of the cell space, the argon was supplied from the bottom outlet ports. Air was exhausted through the upper inlet ports during the inerting operation to reduce the mixing period between air and argon. An additional transition system exchanges the inlet and the outlet ports as necessary to perform this type of inerting operation.

An additional consideration for the suitable positioning of the inlet and the outlet ports can be introduced as in Figure 5. As mentioned above, configurations of the inlet and the outlet ports can affect the entire purging performance of the target facility. In this regard, various positions of the inlet and the outlet should be considered. However, as shown in Figure 5, the argon ports were narrowly arranged concerning the ceiling and both sides of the ground corner in this study because of the requirements of other hot cell components.

3.2. Experiences of Argon Purging for PRIDE Facility

3.2.1. Initial Purging Test of the PRIDE Facility. PRIDE was purged using the combination of dilution and cycle purging methods based on the facility's characteristics while monitoring the oxygen and water concentrations as shown in Figure 6. The entire purging process was as follows. First, argon was charged into the circulation pipes. Subsequently, argon was charged into the PRIDE cell with up to 200 ppm under slightly positive pressure from the ports on the cell's floor. Initially, the dilution was performed for rapid lowering

of the oxygen concentration, and then cycle purging was executed for the high degree of inerting. Finally, the argon purification system was operated to achieve the allowable purity of the facility.

3.2.2. Leakage Test of the PRIDE Facility. A leakage test was also performed using the pressure decay method. The test pressure ranged from approximately -100 mmAq to -30 mmAq under regular operation conditions, and the test volume of the PRIDE cell space was $1,230$ m³. After the test, a leakage check was performed using a sniffer test with 10% Ar or 10% He in the air. As shown in Figure 7, the pressure drop is minimized within the designed time duration.

4. Purging Simulation for the Demonstration-Scale Hot Cell Facility

4.1. Specifications of a Target Facility. The considered hot cell of the target facility is as shown in Figure 8(b); its dimensions are 63, 12, and 10 m. This hot cell comprises several compartments isolated by shielded walls, and the purging system proposed in this study is designed to purge each compartment sequentially. In addition, to simplify the simulation, one of the compartments with horizontal, vertical, and height dimensions of 12, 10, and 4.8 m, respectively, was subjected to a computational fluid dynamic analysis to reduce the simulation load, as shown in Figure 9. Also, only dilution purging was considered in this simulation (cycle purging is not considered).

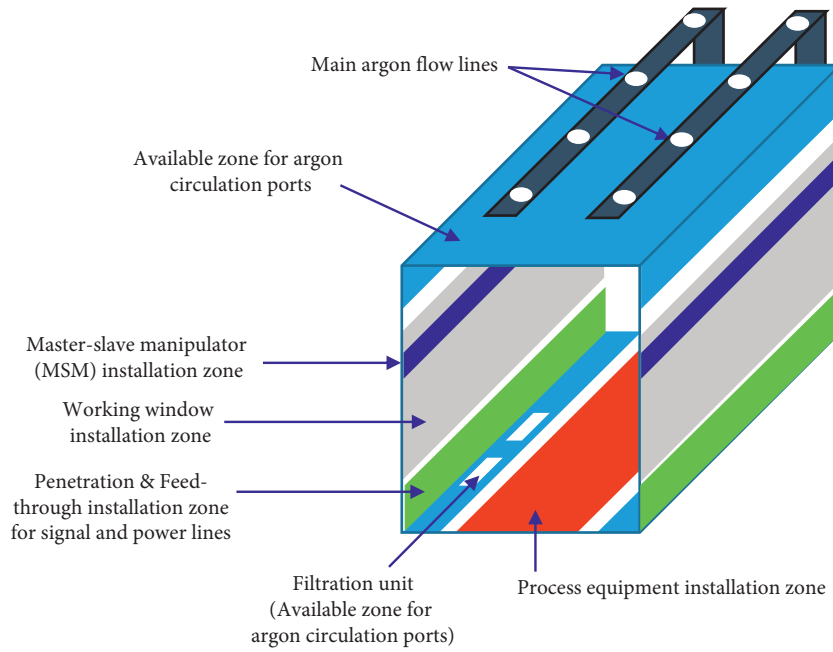


FIGURE 5: Configuration of argon cell of PRIDE facility.

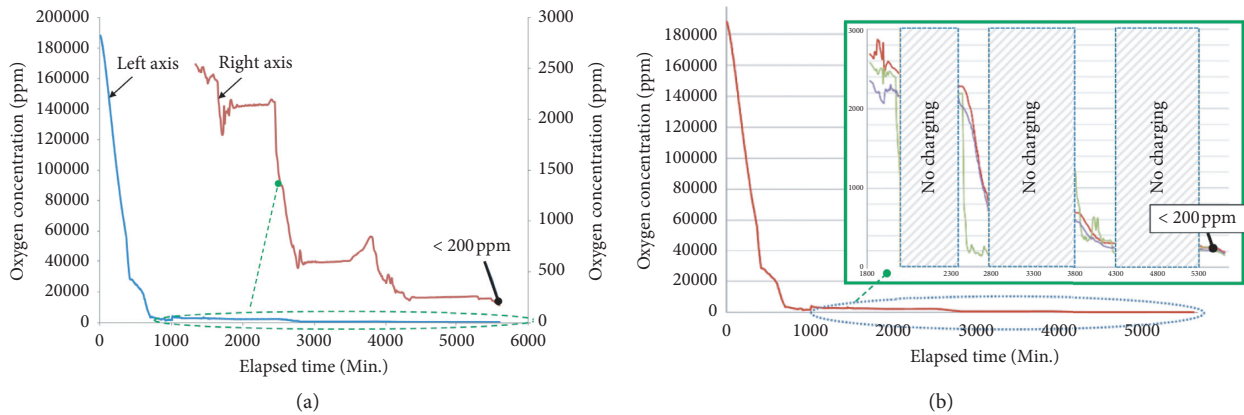


FIGURE 6: Experimental result of purging test for argon cell in PRIDE facility. (a) The result of purging test for argon cell in PRIDE facility. (b) Operational scheme of argon purging test for PRIDE (cycle purging method).

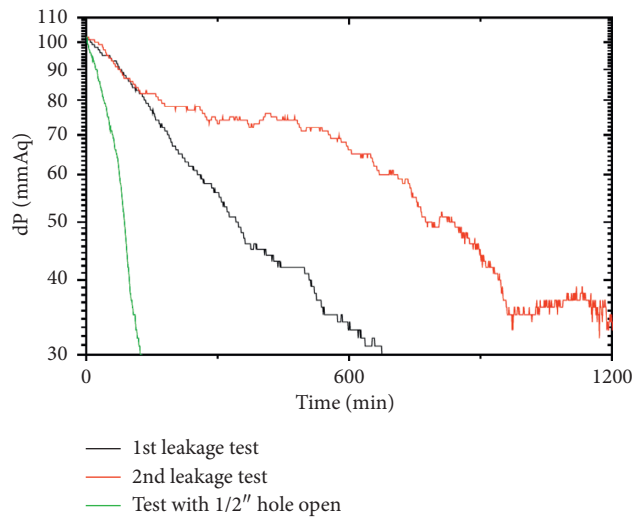
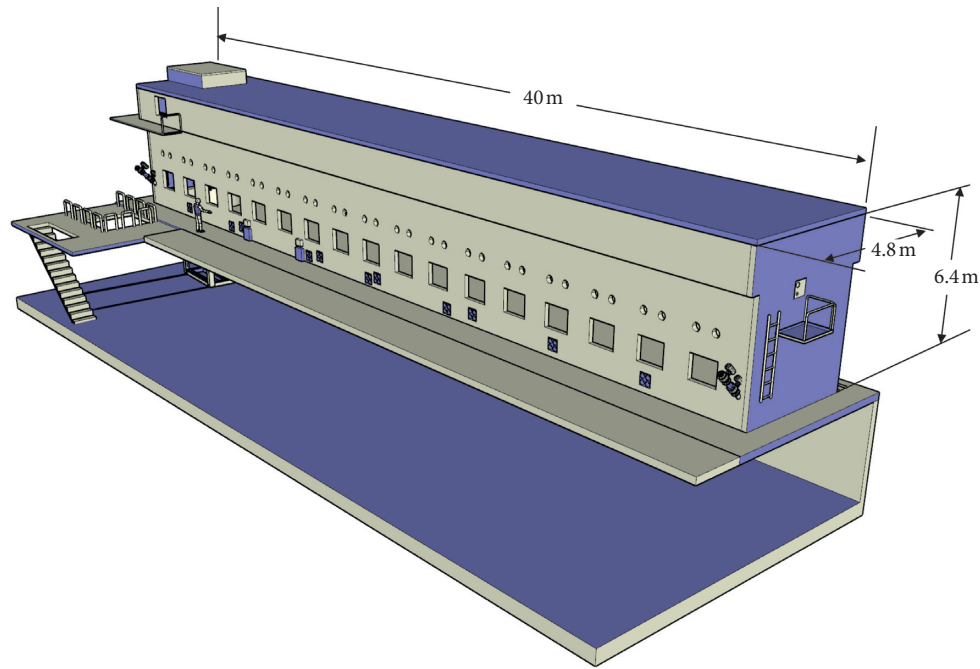
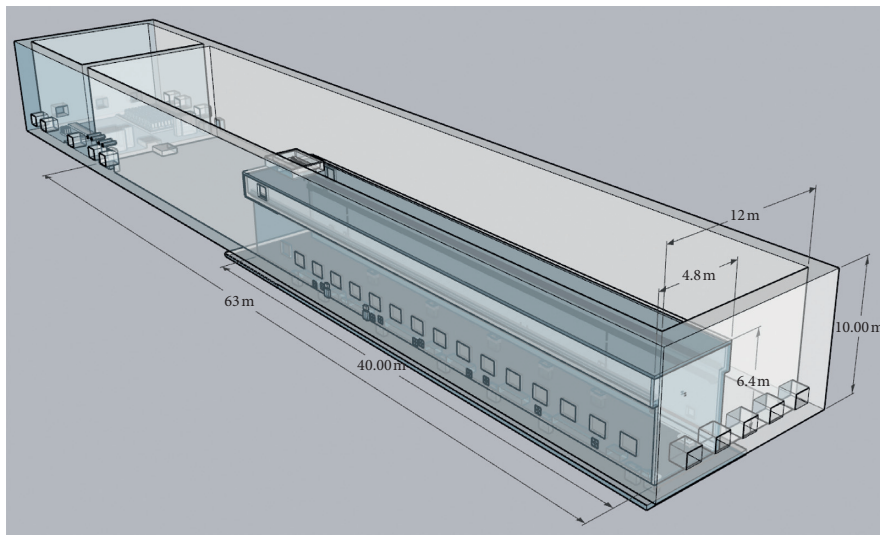


FIGURE 7: Leakage test result for argon cell [23].



(a)



(b)

FIGURE 8: Dimensional comparison of PRIDE (pilot-scale facility) and the target facility (demonstration facility). (a) Dimensions of argon cell in the PRIDE facility. (b) Comparison of dimensions of PRIDE and the target facility.

Before the flow simulation, a comparative analysis was performed between the PRIDE and the target facility of this study with the specifications listed in Table 2.

When the considered demonstration-scale facility is charged initially with argon gas, it is expected to be charged while discharging the air and moisture inside the cell. At this time, the argon gas should be gradually charged to ensure a minimum loss of argon gas. To select the input value of the fluid analysis, the initial charging flow rate is calculated as $7,560 \text{ m}^3/12 \text{ h} = 630 \text{ CMH}$ by considering the volume of the hot cell. However, if the procurement of the actual equipment is considered for the target facility, the initial charging flow

rate is ultimately selected as 600 CMH. In the PRIDE facility, which has one-sixth of the volume of the considered hot cell, it is operated with an initial charging flow rate of approximately 300 CMH for initial purging [23]. Therefore, the 600 CMH of the flow rate could be achieved by double expanding the PRIDE equipment.

4.2. Modeling for Simulation. For the flow simulation, the available designs of the inlet/outlet ports were selected; corresponding dimensions of the inlet and outlet of the target facility are shown in Table 2, and the considered simulation parameters including meshing and time step options are

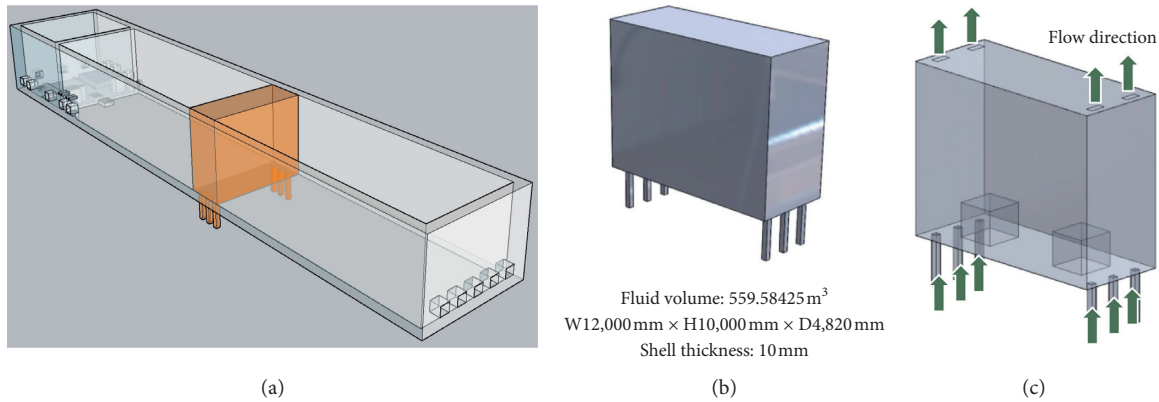


FIGURE 9: Simulation model of the target facility.

TABLE 2: Comparison of PRIDE and the target facility of this study (for regular operation).

Design parameter	PRIDE	Target facility
Cell volume	1,230 m ³	7,560 m ³
No. of inlet ports	20	106
Shape of inlet port	Circular	Square
Area of inlet port	0.033 m ²	0.1008 m ²
Space between inlet ports	Not identified	1.261 m
No. of outlet ports	14	74
Shape of outlet port	Rectangular	Rectangular
Area of outlet port	0.3024 m ²	0.3024 m ²
Space between outlet ports	Not identified	0.952 m

TABLE 3: Parameters for simulation.

Parameters	Values
Simulation type	Internal analysis Time-dependent analysis Gravity effect
Fluid type	Air and argon
Initial pressure	101,325 Pa
Initial temperature	20°C
Initial volume rate	Full air

TABLE 4: Simulation condition of fine meshing with manual time step.

Total no. of mesh	478,496
No. of fluid cells	478,496
No. of fluid cells in contact with solid	103,296

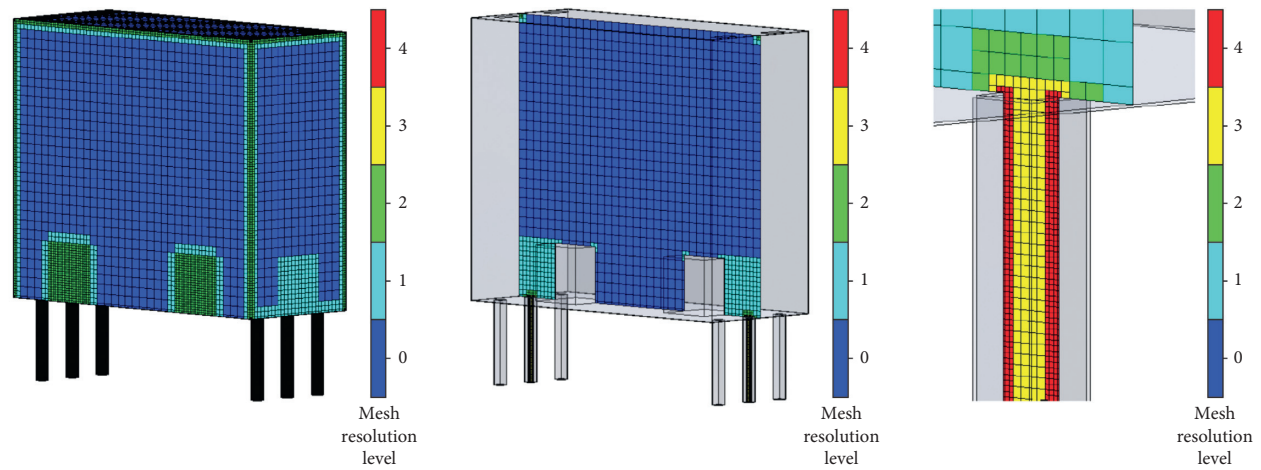
shown in Tables 3–5, respectively. In particular, the meshing approach for the model of the target facility was surveyed for simulation efficiency.

For the efficiency of the computation process, comparison work was initially performed to select an appropriate meshing method and simulation time step, as shown in Figure 10. This

TABLE 5: Simulation condition of coarse meshing with auto time step.

Total no. of mesh	192,588
No. of fluid cells	192,588
No. of fluid cells in contact with solid	61,668

analysis was performed by increasing the input flow rate by 600 and 900 CMH over the previous case of 300 CMH in PRIDE. Essential parameters for inerting, such as temperature and pressure, were assumed to be controlled precisely during the purging process based on the experiences of PRIDE. The presented results of the fine meshing with manual time step versus the coarse meshing with auto time step show a slight error; when the total values are averaged, the volume fraction rate value (average) shows an error of only 3.75%. Also, a manual time step of 0.01 s is the minimum one, whereas the time step of 0.000001 s is displayed depending on the convergence characteristics of the numerical value in which the auto time step is applied; hence, the analysis was performed with a coarse meshing with auto time step to acquire the converged numerical data more efficiently. Table 6 shows the simulation runtime data for the flow rate of 900 CMH according to the type of time step for simulation.



Total cell	192,588
Fluid cell	192,588
Partial cell	61,668

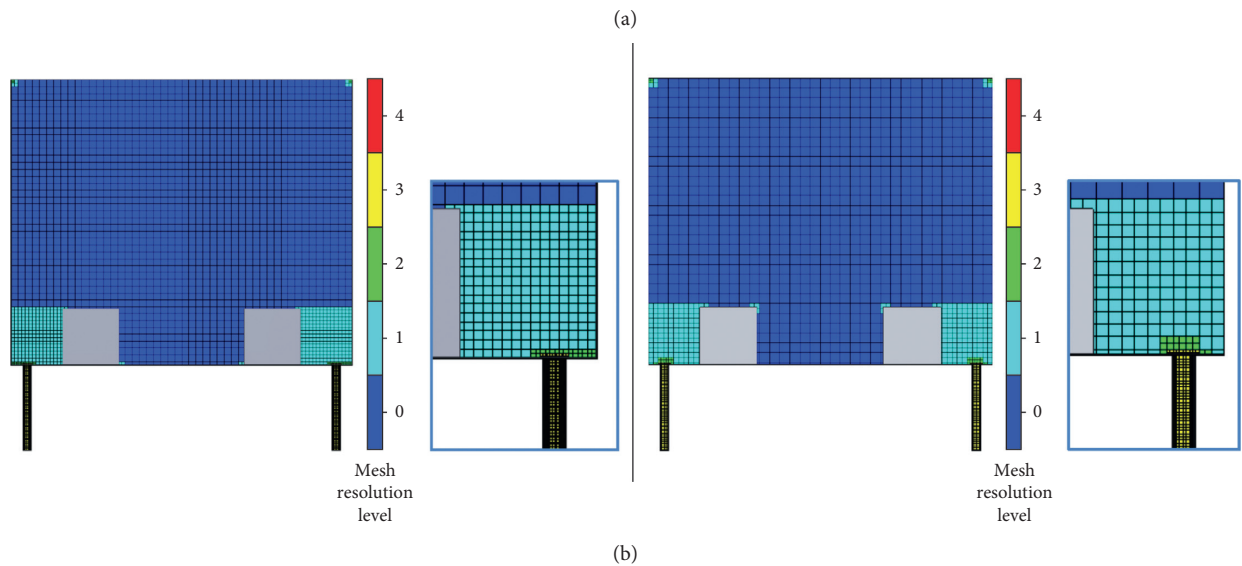


FIGURE 10: (a) Mesh design for the target facility. (b) Comparison of fine and coarse meshes.

TABLE 6: Case of simulation runtime comparison according to time step (auto step vs. manual step; flow rate: 900 CMH).

Contents		99.00%	99.90%	99.95%
		Unit: seconds		
Outlet surface volume fraction of argon, average	Auto step	4,086.76	4,715.83	4,957.90
Outlet surface volume fraction of argon, average	Manual step: (0.06)	3,913.20	4,943.16	5,182.50
Deviation		4%	5%	5%
Outlet surface volume fraction of argon, maximum	Auto step	4,055.52	4,593.66	4,637.52
Outlet surface volume fraction of argon, maximum	Manual step: (0.06)	3,888.24	4,864.68	5,065.32
Deviation		4.12%	5.90%	9.22%
Volume fraction of argon (nine points), average	Auto step	3,465.49	4,184.28	5,116.89
Volume fraction of argon (nine points), average	Manual step: (0.06)	3,260.16	4,359.96	4,970.82
Deviation		5.93%	4.20%	2.85%

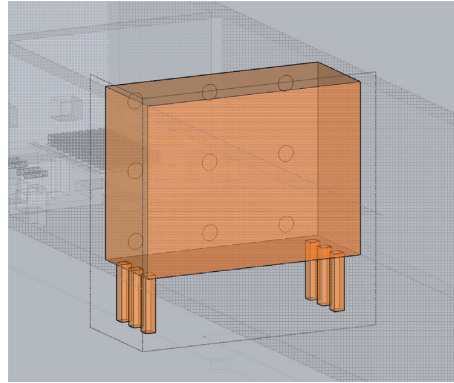


FIGURE 11: Locations for measuring argon volume fraction (nine points).

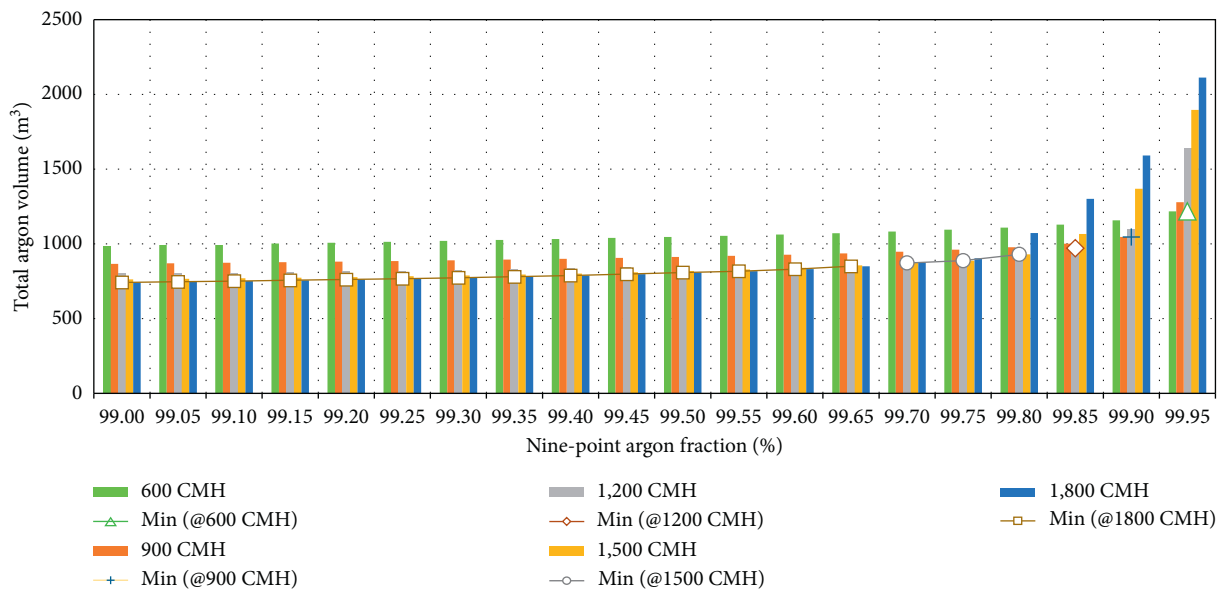


FIGURE 12: Suggestion of flow rate combination for efficient purging, appropriate combination of purging flow rate for argon inerting of the target facility to minimize the total argon volume (“Min(@x CMH)” signifies the flow rate “x” that requires minimized total argon volume among the considered five flow rates to achieve the associated saturation level).

4.3. Simulation Results. The simulation results of the required total argon volume for each argon fraction for nine points (Figure 11) according to the considered flow rate from 600 to 1,800 CMH are summarized in increments of 0.05% from 99.00 to 99.95%, as shown in Figure 12. The flow rate range is selected from the entire simulation data achieved in this study (Figure 13). The required total volume for each argon fraction decreases with a higher flow rate. However, the deviation among the flow rate tends to decrease gradually until around 99.80%. However, in achieving 99.85% saturation, the required total argon volume increases rapidly as the flow rate increases (the higher the flow rate, the greater the internal flow in the final saturation stage). Therefore, to control the total argon volume effectively, it is necessary to predict the optimal trend for each flow rate and apply a variable flow rate

according to the argon fraction of the measuring points. From the data on the chart, the total argon volume required to reach 99.95% saturation decreases with decreasing flow rate. As a result, a high flow rate allows for achieving 99% saturation with the lowest amount of argon. After that, low flow rates have to be applied gradually to reach the final goal of saturation efficiently.

If the variable purging method is unavailable, based on the simulation result of inerting the scale-up facility, a single value of the purging rate should be selected. As shown in Figure 14, a flow rate higher than 600 CMH may not be preferable in this study; this is because more argon is required to reach the final goal of 99.95% saturation at the nine designated points (Figure 11) inside the hot cell when the flow rate is 900 CMH than when it is 600 CMH.

	Target Achieve Time (S) Chart	99.00%	99.05%	99.10%	99.15%	99.20%	99.25%	99.30%	99.35%	99.40%	99.45%	99.50%	99.55%	99.60%	99.65%	
600	Outlet Surface Volume Fraction of Argon - Average	6938.9														7359.16
600	Outlet Argon Fraction (Avg.) - Total Argon Volume	1156.4														1226.53
600	Outlet Surface Volume Fraction of Argon - Maximum	6898.2														7300.29
600	Outlet Argon Fraction (Max.) - Total Argon Volume	1149.7														1216.72
600	Volume Fraction of Argon - 9 Point Avg	5925.0														6431.15
600	9P Argon Fraction - Total Argon Volume	987.5														1071.86
900	Outlet Surface Volume Fraction of Argon - Average	4086.7														4377.10
900	Outlet Argon Fraction (Avg.) - Total Argon Volume	1021.6														1094.28
900	Outlet Surface Volume Fraction of Argon - Maximum	4055.5														4325.55
900	Outlet Argon Fraction (Max.) - Total Argon Volume	1013.8														1081.39
900	Volume Fraction of Argon - 9 Point Avg	3465.4														3747.19
900	9P Argon Fraction - Total Argon Volume	866.3														936.80
1200	Outlet Surface Volume Fraction of Argon - Average	2871.4														3084.93
1200	Outlet Argon Fraction (Avg.) - Total Argon Volume	957.1														1028.31
1200	Outlet Surface Volume Fraction of Argon - Maximum	2838.9														3029.26
1200	Outlet Argon Fraction (Max.) - Total Argon Volume	946.3														1009.75
1200	Volume Fraction of Argon - 9 Point Avg	2403.7														2635.62
1200	9P Argon Fraction - Total Argon Volume	801.2														878.54
1500	Outlet Surface Volume Fraction of Argon - Average	2210.4														2393.99
1500	Outlet Argon Fraction (Avg.) - Total Argon Volume	921.0														997.50
1500	Outlet Surface Volume Fraction of Argon - Maximum	2181.7														2286.46
1500	Outlet Argon Fraction (Max.) - Total Argon Volume	909.0														952.69
1500	Volume Fraction of Argon - 9 Point Avg	1830.1														2054.49
1500	9P Argon Fraction - Total Argon Volume	762.5														856.04
1800	Outlet Surface Volume Fraction of Argon - Average	1798.7														1943.25
1800	Outlet Argon Fraction (Avg.) - Total Argon Volume	899.3														971.63
1800	Outlet Surface Volume Fraction of Argon - Maximum	1766.0														1903.76
1800	Outlet Argon Fraction (Max.) - Total Argon Volume	883.0														951.88
1800	Volume Fraction of Argon - 9 Point Avg	1485.1														1701.30
1800	9P Argon Fraction - Total Argon Volume	742.5														850.65

FIGURE 13: Simulation results of the total volume to achieve the nine-point argon fraction for the entire range of flow rates considered in this study (from 600 to 12,000 CMH) and selected range of flow rates for a suggestion.

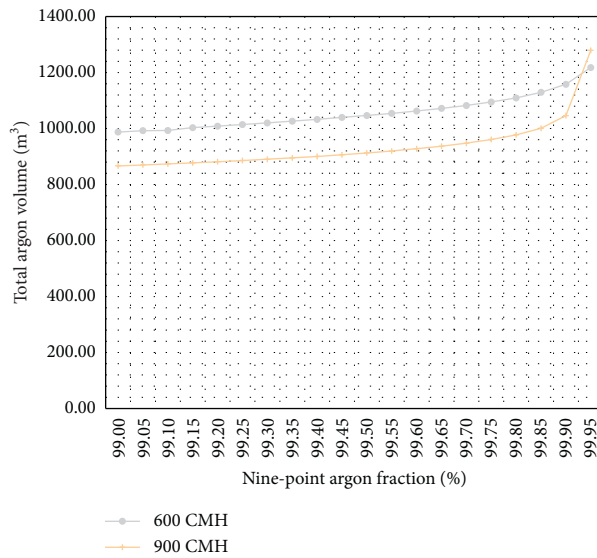


FIGURE 14: Total argon volume to achieve the nine-point argon fraction (see Figure 11).

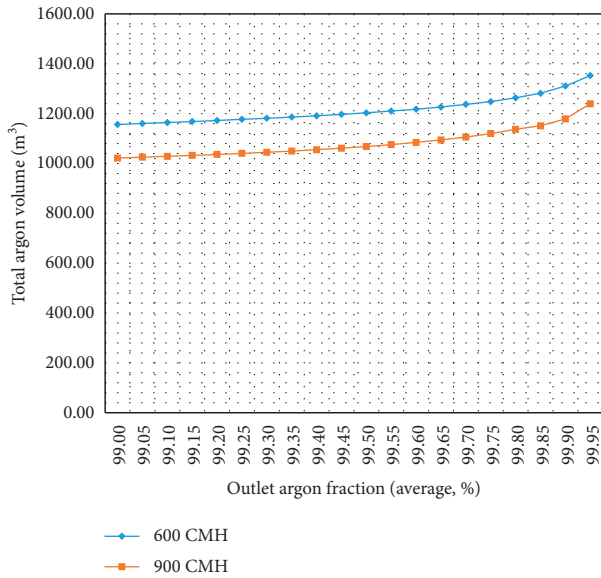


FIGURE 15: Total argon volume to achieve the outlet argon fraction (average).

Furthermore, as shown in Figure 15, to reduce the total argon volume by 20% while achieving the same argon fraction at the outlet, the purging flow rate should be increased by 50%, and the efficiency decreases with the higher argon fraction of the outlet, resulting in a drop in the efficiency of the argon purging system. Based on the simulation results of inerting the scale-up facility, a purging flow rate of approximately 600 CMH would be more appropriate than a higher flow rate input for single-rate purging.

5. Conclusions and Considerations

5.1. Conclusions. This study primarily focused on the conceptual design of a demonstration-scale hot cell facility beyond the currently existing pilot-scale hot cell facility. For this purpose, practical constraints for the CFD simulation were introduced based on experiences garnered from the existing pilot-scale facility. The approach taken in this study was as follows:

- (1) To determine the proper purging rate for the initial inerting of a demonstration-scale hot cell facility, we analyzed the operation case of a currently operating pilot-scale argon cell facility, “PRIDE”
- (2) We compared and analyzed the various inerting methods for industrial applications
- (3) Based on the analysis of cases of industry and the PRIDE facility, we selected the proper inerting media and range of initial purging rates for the target facility
- (4) We simulated various purging rates for inerting and compared each simulation case
- (5) Finally, we proposed the proper combination of flow rates for the initial purging of the demonstration-scale hot cell facility

Input parameters for simulation, such as flow rates, were calculated by considering the existing facility’s specifications to secure the feasibility of this study. We investigated the upper range of flow rates for the larger-scale facility by incrementally applying the flow rates. However, in this study, since the simulation was performed on the hot cell, which has a specific size, it is necessary to analyze and verify the various sizes of hot cells in order to achieve sufficient validity. This will be included in the future work of this study.

Despite the abovementioned limitation, the results of this study, such as the purging method with variable flow rate, can be helpful in the design of larger-scale hot cell facilities operated under inert conditions.

5.2. Considerations. Based on the results of this study, the inert gas purged into the hot cell for regular operation can be a function of the demand. Generally, the level of demand is based on maintaining a specified pressure within the hot cell against the surrounding atmosphere. The variable application introduces an advantageous approach over consistent application in that the inert gas can be supplied only when required to reduce: (1) the total amount of the inert gas required, (2) the loss of inert gas, and (3) the waste for disposal. The challenge is the dependence on flow control devices operated by very low-pressure differentials that are sometimes difficult to manage. For the variable-rate application of initial purging and regular operation, an inerting system is required to monitor such an atmosphere in the considered space. Technically, this system should include an automatic inert-gas supply valve or regulator to control the oxygen concentration below the considered limit of oxygen concentration. This kind of control system should equip an analyzer to monitor the oxygen concentration continuously and allow the inert gas to purge the space to maintain the oxygen concentration at safe levels with an acceptable margin of safety [24]. An increase in the concentration above the set point (for regular operation) or a decrease in the concentration below the set point (for initial purging) should initiate an alarm or control of the flow rate.

Another important consideration is that the minimum achievable oxygen concentration depends on the purity of the inert gas, the facility’s gas-tight integrity, and the presence of back diffusion from the exhaust line. Therefore, it is necessary to continue to supply inert gas even after attaining the desired oxygen level to maintain a given oxygen concentration, as the operational case of PRIDE.

Data Availability

The data used to support the findings of this study are available from the corresponding author upon reasonable request.

Conflicts of Interest

The authors declare that they have no conflicts of interest regarding the publication of this paper.

Acknowledgments

This work was partly supported by the Korea Institute of Energy Technology Evaluation and Planning (KETEP) grant funded by the Korean government (MOTIE) (202015203000090) and also supported by the Nuclear Research & Development Program of the National Research Foundation of Korea (NRF) funded by the Ministry of Science, ICT and Future Planning (MSIP).

References

- [1] K.-C. Song, H.-S. Lee, J.-M. Hur, J.-G. Kim, D.-H. Ahn, and Y.-Z. Cho, "Status of pyroprocessing technology development in Korea," *Nuclear Engineering and Technology*, vol. 42, no. 2, pp. 131–144, 2010.
- [2] H. Lee, J.-M. Hur, J.-G. Kim, D.-H. Ahn, Y.-Z. Cho, and S.-W. Paek, "Korean pyrochemical process R&D activities," *Energy Procedia*, vol. 7, pp. 391–395, 2011.
- [3] J. H. Ku, S. I. Moon, I. J. Cho, W. M. Choung, G. S. You, and H. D. Kim, "Development of pyroprocess integrated inactive demonstration facility," *Procedia Chemistry*, vol. 7, pp. 779–784, 2012.
- [4] S. Yu, J. Lee, B. Park, I. Cho, and H. Lee, "Design considerations for teleoperation systems operating in gas-tight argon cells," *Nuclear Engineering and Technology*, vol. 49, no. 8, pp. 1717–1726, 2017.
- [5] H. Lee, G. I. Park, J. W. Lee et al., "Current status of pyroprocessing development at KAERI," *Science and Technology of Nuclear Installations*, vol. 2013, Article ID 343492, 11 pages, 2013.
- [6] H. J. Lee, W. I. Ko, I. T. Kim, and H. S. Lee, "Design for integrated pyroprocessing plant level simulator," *Annals of Nuclear Energy*, vol. 60, pp. 316–328, 2013.
- [7] H. J. Lee, J. K. Lee, B. S. Park, K. Kim, W. I. Ko, and I. J. Cho, "Development of a remote handling system in an integrated pyroprocessing facility," *International Journal of Advanced Robotic Systems*, vol. 10, no. 10, p. 345, 2013.
- [8] S. Yu, J. Lee, B. Park, K. Kim, and I. Cho, "Ergonomic analysis of a telemanipulation technique for a pyroprocess demonstration facility," *Nuclear Engineering and Technology*, vol. 46, no. 4, pp. 489–500, 2014.
- [9] I. J. Cho, J. H. Sim, and Y. S. Kim, "Quantitative evaluation of radiation dose rates for depleted uranium in PRIDE facility," *Journal of Radiation Protection and Research*, vol. 41, no. 4, pp. 378–383, 2016.
- [10] H. Seo, C. Lee, S. K. Lee et al., "Development of PRIDE UNDA for safeguards application," *Journal of Nuclear Science and Technology*, vol. 53, no. 6, pp. 878–886, 2016.
- [11] D. Gertenbach and B. Cooper, *Scale-up Issues from Bench to Pilot*, American Institute of Chemical Engineers National Meeting, Nashville, TN, India, 2009.
- [12] Website: <http://www.matricinnovates.com/matric-matters-blog/defining-pilot-plant-objectives-understanding-implications/>.
- [13] W. F. Holcomb, D. M. Paige, and L. F. Coleman, "Operating experience with the EBR-II fuel cycle facility inert atmosphere cell," *Nuclear Applications*, vol. 2, no. 3, pp. 254–255, 1966.
- [14] K. M. Goff, J. C. Wass, K. C. Marsden, and G. M. Teske, "Electrochemical processing of used nuclear fuel," *Nuclear Engineering and Technology*, vol. 43, no. 4, pp. 335–342, 2011.
- [15] D. B. Hagmann and A. A. Chilenskas, *Conceptual Design for the Handling and Remote Disassembly of the Fuel Element Failure Propagation Loop at the HFEF (No. ANL/HFEF-1)*, Argonne National Lab., Idaho Falls, ID, USA, 1972.
- [16] S. D. Herrmann, *Pilot-scale Equipment Development for Pyrochemical Treatment of Spent Oxide Fuel (No. ANL/NT/CP-98166)*, Argonne National Lab., Lemont, IL, USA, 1999.
- [17] B. S. Park, J. K. Lee, S. N. Yu, K. H. Him, and I. J. Cho, "Construction of ACPF hot cell Argon compartment system," in *Proceedings of the 2014 Korean Radioactive Waste Society Autumn Meeting*, pp. 127–128, Yeosu, Republic of Korea, October 2014.
- [18] S. N. Yu, J. K. Lee, B. S. Park, I. Cho, and K. Kim, "Hot cell renovation in the spent fuel conditioning process facility at the Korea atomic energy research institute," *Nuclear Engineering and Technology*, vol. 47, no. 6, pp. 776–790, 2015.
- [19] J. Han, W. K. Lee, D. H. Hong, and I. J. Cho, "Pre-operation tests of a pyroprocess integrated inactive demonstration facility," in *Proceedings of the 50th Annual Meeting on Hot Laboratories and Remote Handling (HOTLAB 2013)*, Idaho Falls, ID, USA, September 2013.
- [20] ISO 17873, *Nuclear Facilities- Criteria for the Design and Operation of Ventilation Systems for Nuclear Installations Other than Nuclear Reactors*, International Organization for Standardization, Geneva, Switzerland, 2004.
- [21] H. J. Reinhardt and H. R. Himmen, *Inerting in the Chemical Industry*, Hydrocarbon Processing, Pullach, Germany, 2010.
- [22] Matheson Tri-Gas, *Instruction Manual- Purging High Purity Gas Delivery Systems*, Matheson, Irving, TX, USA, 1927.
- [23] I. J. Cho, "PRIDE's system for engineering-scale pyroprocessing development," in *Proceedings of the 2012 International Pyroprocessing Research Conference (IPRC 2012)*, Madison, WI, USA, August 2012.
- [24] J. Lee, A. Shigrekar, and R. A. Borrelli, "Application of hazard and operability analysis for safeguardability of a pyroprocessing facility," *Nuclear Engineering and Design*, vol. 348, pp. 131–145, 2019.